



HAL
open science

Discrete Geodesics and Cellular Automata

Pablo Arrighi, Gilles Dowek

► **To cite this version:**

Pablo Arrighi, Gilles Dowek. Discrete Geodesics and Cellular Automata. Theory and Practice of Natural Computing, Dec 2015, Mieres, Spain. 10.1007/978-3-319-26841-5_11 . hal-01252131

HAL Id: hal-01252131

<https://inria.hal.science/hal-01252131>

Submitted on 7 Jan 2016

HAL is a multi-disciplinary open access archive for the deposit and dissemination of scientific research documents, whether they are published or not. The documents may come from teaching and research institutions in France or abroad, or from public or private research centers.

L'archive ouverte pluridisciplinaire **HAL**, est destinée au dépôt et à la diffusion de documents scientifiques de niveau recherche, publiés ou non, émanant des établissements d'enseignement et de recherche français ou étrangers, des laboratoires publics ou privés.

Discrete geodesics and cellular automata

Pablo Arrighi¹ and Gilles Dowek²

¹ Aix-Marseille Univ., LIF, F-13288 Marseille Cedex 9, France
pablo.arrighi@univ-amu.fr,

² Inria, 23 avenue d'Italie, CS 81321, 75214 Paris Cedex 13, France.
gilles.dowek@inria.fr

Abstract. This paper proposes a dynamical notion of discrete geodesics, understood as straightest trajectories in discretized curved spacetime. The notion is generic, as it is formulated in terms of a general deviation function, but readily specializes to metric spaces such as discretized pseudo-riemannian manifolds. It is effective: an algorithm for computing these geodesics naturally follows, which allows numerical validation—as shown by computing the perihelion shift of a Mercury-like planet. It is consistent, in the continuum limit, with the standard notion of timelike geodesics in a pseudo-riemannian manifold. Whether the algorithm fits within the framework of cellular automata is discussed at length.

Keywords: Discrete connection, parallel transport, general relativity, Regge calculus.

1 Introduction

Three reasonable hypotheses—bounded velocity of propagation of information, homogeneity in time and space, and bounded density of information—lead to the thesis that natural phenomena can be described and simulated by cellular automata. This implication has in fact been formalized into a theorem both in the classical [9] and the quantum case [1], albeit in flat space. Further evaluating this thesis leads to the project of selecting specific physical phenomena, such as gravitation, and attempting to describe them as cellular automata. A first step in this direction is to build discrete models of the phenomena. In the case of gravitation, this leads to the question we address in this paper: what is a discrete geodesics?

Geodesics generalize the flat space notion of line, to curved spaces. A line is both the shortest, and the straightest path between two points, but in curved space the two criteria do not coincide [12]. In computer graphics and discrete geometry, discrete geodesics as shortest path between two given point have been studied extensively [13, 14]. This is not the case of geodesics as straightest path given an initial point and velocity—with the noticeable exception of [15], in the framework of simplicial complexes. Yet, it is this criterion that one must adopt in order to describe and simulate the timelike geodesics trajectories of particles. In this paper we adopt the dynamical, spacetime view on geodesics which is typical of numerical relativity [16]. But instead of discretizing geodesics defined

by partial differential equations in a continuous spacetime, we seek to discrete geodesics as a native notion of a discretized spacetime, for instance of a grid endowed with a metric.

More precisely, the paper proposes both a notion of discrete-spacetime geodesics and a notion of discrete-time continuous-space geodesics (Section 2). Both are generic, that is formulated in terms of a general deviation function, but readily specialize for metric spaces (Section 4). They are effective: an algorithm for computing timelike geodesics naturally follows (Section 3), which allows us to validate the notions numerically, by computing the perihelion shift of a Mercury-like planet (Section 5). They are consistent with one another: the former is clearly a discretization the the latter. Moreover, the latter is proven to have the standard notion of continuous-spacetime geodesics in a Riemannian space as its limit, which validates both notions as legitimate discrete counterparts (Section 9). Whether the algorithm fits within the framework of cellular automata is discussed at length, as well as how this impacts on precision (Sections 6-8).

These results apply to natively discrete formulations of General Relativity such as Regge calculus [17, 4]. For instance, our method yields perihelion shift computations of the right order, an issue in [17] pointed out in [4]. We discuss how our approach differs from [15] and why it fixes this issue. Finally, an often underestimated contribution is the pedagogical: the simple discrete model summarized in Figure 1 has continuum limit the complicated, well-known equations of (9) and (10).

Besides assessing this “digital physics” program, we believe that these results can be applied in any inherently discrete geometrical setting, in order to compute geodesics without the need to interpolate a continuous surface. Such applications may arise in computer vision and graphics [14] including computer anatomy [10].

2 Discrete geodesics

Consider a discrete-time continuous-space spacetime $\mathbb{Z} \times \mathbb{R}^n$ where \mathbb{Z} is the discrete timeline and \mathbb{R}^n a continuous space. Consider a *deviation* function w from $(\mathbb{Z} \times \mathbb{R}^n)^3$ to \mathbb{R}^+ , the number $w(E, F, G)$ measuring how the path E, F, G deviates from “going straight ahead”. In this setting, a *geodesic* is a sequence of points in $\mathbb{Z} \times \mathbb{R}^n$ $(E_i)_i$ such that for any i , $w(E_{i-1}, E_i, E_{i+1}) = 0$. Such a property can be read as a condition on E_{i+1} : if the points E_{i-1} and E_i are given, the geodesics must continue with a point E_{i+1} such that $w(E_{i-1}, E_i, E_{i+1}) = 0$.

Consider now a discrete spacetime $M = \mathbb{Z} \times \mathbb{Z}^n$ where \mathbb{Z} is the discrete timeline and \mathbb{Z}^n a discrete space and a deviation function w from M^3 to \mathbb{R}^+ which, as above, measures how the path E, F, G deviates from going straight ahead. In this setting we cannot demand $w(E_{i-1}, E_i, E_{i+1})$ to be exactly zero, but we demand that it be a minimum with respect to *spatial local variations* of E_{i+1} .

Spatial local variations can be defined as follows. Let us write $\langle x_0, x_1, \dots, x_n \rangle$, the coordinates of a point E in M , where x_0 is the time coordinate and x_1, \dots, x_n

the space coordinates. Two points of M , $\langle x_0, x_1, \dots, x_n \rangle$ and $\langle x'_0, x'_1, \dots, x'_n \rangle$ are said to be *spatial neighbors* if $x_0 = x'_0$ and for all $i \geq 1$, $|x'_i - x_i| \leq 1$.

Thus, a *discrete geodesics* in M can be defined as a sequence of points in M , $(E_i)_i$ such that for any i , the deviation $w(E_{i-1}, E_i, E_{i+1})$ is a local minimum with respect to spatial local variations of E_{i+1} , that is for any spatial neighbor G of E_{i+1} , we have

$$w(E_{i-1}, E_i, G) \geq w(E_{i-1}, E_i, E_{i+1}) \quad (1)$$

Notice how this condition may be understood as a discrete counterpart of the Euler-Lagrange equation, in the spirit of [11].

3 An algorithm to compute a geodesic

We now give a gradient descent-like algorithm to compute a discrete geodesic, $\langle t_0, A_0 \rangle, \langle t_1, A_1 \rangle, \langle t_2, A_2 \rangle$ given a deviation function w , a timeline t_0, t_1, t_2, \dots , and two starting points A_0 and A_1 .

Assume, A_{i-1} and A_i are computed. To compute A_{i+1} start with a point $\langle t_{i+1}, C \rangle$. Compute $w(\langle t_{i-1}, A_{i-1} \rangle, \langle t_i, A_i \rangle, \langle t_{i+1}, C' \rangle)$ for all 3^n spatial neighbour C' of C . If they are all larger than $w(\langle t_{i-1}, A_{i-1} \rangle, \langle t_i, A_i \rangle, \langle t_{i+1}, C \rangle)$ take C for A_{i+1} . Otherwise chose a C' which minimizes $w(\langle t_{i-1}, A_{i-1} \rangle, \langle t_i, A_i \rangle, \langle t_{i+1}, C' \rangle)$ and iterate, starting from this C' .

Whether this iteration will eventually end depends, in general, on $w(\cdot, \cdot, \cdot)$. For instance, say that $w(\langle t_{i-1}, A_{i-1} \rangle, \langle t_i, A_i \rangle, \langle t_{i+1}, C' \rangle)$ increases as soon as $A_i C' > t_{i+1} - t_i$. Then A_{i+1} will have to lie within distance $t_{i+1} - t_i$ of A_i , thereby imposing a bounded velocity $c = 1$, as well as enforcing termination.

4 Distance induced deviation function

Most of the times, the idea of deviating from going straight is induced from a notion of distance. Here is how. Suppose a distance function d , and define the three point distance function

$$l(E, F, G) = d(E, F) + d(F, G).$$

Intuitively, **FG** is understood to deviate from **EF** if it “leans” in some spatial direction **FF'**, as witnessed by the fact that

$$l(E, F', G) < l(E, F, G)$$

for F' some neighbour of F .

In a continuous-space discrete-time setting this would be formalized by letting $w(E, \langle x_0, \dots, x_n \rangle, G)$ be

$$\partial_0 l(E, \langle x_0, \dots, x_n \rangle, G)^2 + \dots + (\partial_n l(E, \langle x_0, \dots, x_n \rangle, G))^2. \quad (2)$$

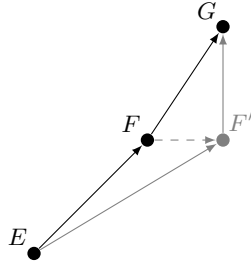


Fig. 1. Discrete geodesics seek to find G such that \mathbf{FG} minimizes its deviation relative to \mathbf{EF} . In the case of metric spaces, \mathbf{FG} is understood to “deviate towards \mathbf{FF}' relative to \mathbf{EF} ”, whenever $l(E, F', G) < l(E, F, G)$ —such deviations must be minimized.

Thus, for continuous-space discrete-time geodesics $(E_i)_i$ each point E_i is a local extremum for $l(E_{i-1}, E_i, E_{i+1})$.

In the discrete spacetime case, $w(E, \langle x_0, \dots, x_n \rangle, G)$ is simply obtained by replacing partial derivatives with finite differences in Equation (2): $\partial_\mu l(E, \langle x_0, \dots, x_n \rangle, G)$ becomes

$$(l(E, \langle x_0, \dots, x_\mu - 1, \dots, x_n \rangle, G) - l(E, \langle x_0, \dots, x_\mu + 1, \dots, x_n \rangle, G))/2. \quad (3)$$

And, for discrete spacetime geodesics $(E_i)_i$ each point E_i minimizes the possibly non-zero $w(E_{i-1}, E_i, E_{i+1})$.

5 Discrete Schwarzschild spacetime

In this section, we give an example of discrete spacetime, which is a discretization of the Schwarzschild spacetime of General Relativity.

Discretize spacetime down to $\Delta = 1cm$. Consider a star of mass $M = 2.10^{30}kg$ —like the Sun. Its Schwarzschild radius is $m = 2\mathcal{G}M/c^2 = 3km = 3.10^5cm$. In order to evaluate distances, consider the metric tensor

$$g(\langle t, x, y \rangle) = \begin{pmatrix} 1 - \frac{m}{r} & 0 & 0 \\ 0 & -\frac{x^2}{r(r-m)} - \frac{y^2}{r^2} & -\frac{mxy}{r^2(r-m)} \\ 0 & -\frac{mxy}{r^2(r-m)} & -\frac{x^2}{r^2} - \frac{y^2}{r(r-m)} \end{pmatrix}$$

where $r = \sqrt{x^2 + y^2}$, and let the distance function d be defined by

$$d(E, F) = \sqrt{\mathbf{EF}^\dagger g(E)\mathbf{EF}}.$$

We study the geodesics trajectory of a planet, with respect to a timeline $0, \tau, 2\tau, 3\tau, \dots$ with $a = 10^7$ and $\tau = a\Delta$. Thus $\tau = 10^7cm = 3.33 \cdot 10^{-4}s$. The fake planet has parameters chosen so as to maximize relativistic effects: its first

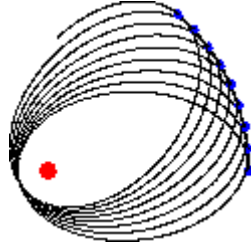


Fig. 2. The computed trajectory of a planet.

point is $E = \langle x_0 = 0, x_1 = 10^8 \text{cm} = 1000 \text{km}, x_2 = 0 \rangle$, and its initial velocity is $v_x = 0, v_y = 2 \cdot 10^{-2} c = 6000 \text{km} \cdot \text{s}^{-1}$.

We compute the geodesics with respect to the $w(\cdot, \cdot, \cdot)$ induced by $d(\cdot, \cdot)$ as in Section 4, and following the algorithm of Section 3. Recall that in this algorithm at iteration i the point A_{i+1} is found by gradient descent starting from some point C . In the context of planetary movement, a good guess for C is obtained as follows. Define velocity $S_i = A_i - A_{i-1}$ and acceleration $R_i = S_i - S_{i-1}$, and make the guess that acceleration will remain constant, that is $R_{i+1} = R_i$. This would entail that $A_{i+1} = A_i + S_i + R_i$, thus take $C = A_i + S_i + R_i$ as the first guess and start exploring for the real A_{i+1} . Within reasonable ranges other heuristics—for instance, $C = A_i + S_i$ —lead to the same trajectories, but may require longer computation times.

A run of the simulation is shown in Figures 2 and 3. Computation time is a few seconds. The code is available in [2]. The code is easily augmented to detect aphelion, typically $a = 1000 \text{km}$, and perihelion, typically $p = 150 \text{km}$.

The perihelion shift is visible on Figure 2. A well-known formula [8] states that perihelion shift in radians per revolution should be

$$\sigma = \frac{24\pi^3 L^2}{T^2 c^2 (1 - e^2)} = \frac{6\pi \mathcal{G}M}{c^2 L (1 - e^2)} = \frac{3\pi m}{P}$$

where T is the revolution period of the planet, L is the semi-major axis of the trajectory of the planet, e its eccentricity, and $P = L(1 - e^2)$ its parameter—recall that, by Kepler's third law, $T^2 = 4\pi^2 L^3 / (\mathcal{G}M)$, and $m = 2\mathcal{G}M/c^2$. Then an easy geometrical relation is

$$P = \frac{2}{1/a + 1/p}$$

hence

$$\sigma = (3/2)\pi m(1/a + 1/p)$$

which typically is 6.17 deg. The observed shift is around 6.27 deg.

```

Perihelion
t = 3580000000 cm x = -15031004 cm y = -1398397 cm
angle = -174.6849818385271 deg
distance = 1.5095913202506995E7 cm
velocity = 0.13034045668302685 c
-----
Aphelion
t = 7150000000 cm x = 99552205 cm y = 11035292 cm
angle = 6.325378791430483 deg
distance = 1.0016196478647615E8 cm
velocity = 0.019968511905497616 c
theoretical shift = 6.174380835177214 deg
observed shift = 6.210787288401395 deg
-----
Perihelion
t = 10730000000 cm x = -14847048 cm y = -2698767 cm
angle = -169.69789787187233 deg
distance = 1.5090333913952766E7 cm
velocity = 0.13035029101632262 c
-----
Aphelion
t = 14310000000 cm x = 97909925 cm y = 21872062 cm
angle = 12.592542500595265 deg
distance = 1.0032318032058926E8 cm
velocity = 0.019937902185786747 c
theoretical shift = 6.175065136027821 deg
observed shift = 6.267163709164782 deg

```

Fig. 3. Numerics of the computed trajectory of a planet.

6 Cellular Automata in Mechanics

As suggested in the Introduction, one motivation for discretizing General Relativity is to describe the motion of a planet in a cellular automaton.

Recall that, in the cellular automata vocabulary, a configuration σ is a function which associates, to each cell C of the grid \mathbb{Z}^n , some internal state $\sigma(C)$ taken in the set Σ . A cellular automaton is a function F from configurations to configurations, which has the following physics-inspired symmetries:

- bounded velocity of propagation of information;
- homogeneity time and space;
- bounded density of information, that is Σ is finite.

The state of a cell can be used to express the presence or the absence of a particle in this region of space. This way cellular automata can describe particle motions. For instance the simplest n -dimensional cellular automata—2 states,

radius 1—can describe one particle motion among 3^n , as in each dimension, it could have velocity -1 , 0 , or 1 .

To describe more complex motions, we must increase the number of states. For instance in a 1-dimensional automaton with radius 1, we can describe the motion of a particle that goes to the right at velocity $1/2$, by alternating states s_1 —stay still—and s_2 —step—, but also the motion of a particle that goes to the right at velocity 1, staying in the state s_3 .

Another option is to increase the radius of the automaton. For instance, in a 1-dimensional automaton, with radius 2 we can describe the motion of a particle that goes on the right at velocity 1 staying in a state s_1 or at velocity 2 staying in a state s_2 . Notice that modulo changing the units, the former behaviour can be obtained from the latter just by cell grouping.

We want to address the following question: to what extent is the algorithm of Section 3 just a cellular automaton?

7 Geodesics as Cellular Automata

Whether the algorithm of Section 3 enforces a bounded velocity of propagation of information $c = 1$ depends, in general, on the properties of $w(., ., .)$. If such a velocity bound is enforced, then the motion of the body can be described in a cellular automaton of radius r . It is well-known that the velocity of a particle in a continuous Schwarzschild spacetime is bounded by $c = 1$. We conjecture that this is also the case for the discretized Schwarztchild spacetime.

If $w(., ., .)$ does not depend on space and time, then the algorithm clearly acts the same everywhere and everywhen, so that homogeneity is also enforced. In the important case where it depends upon a space-dependent metric, then this metric field has to be carried by the internal state of the cells, even if it does not contain a particle, so that homogeneity is still enforced.

Let us evaluate whether bounded density of information holds. Even when $w(., ., .)$ does not depend on space and time, it is still the case that if a particle is at E_i , we need its velocity $\mathbf{E}_{i-1}\mathbf{E}_i$ to compute its next position E_{i+1} . But thanks to bounded velocity of propagation, and the fact that positions are discrete, the number of possible velocities is bounded above by $b = (2a+1)^n$, so that bounded density of information is preserved. In the important case of a space-dependent metric carried by the internal state of the cells, whether bounded density holds depends upon whether we can assume that the metric field can be given with bounded precision. Even if this is not the case, notice that for a given cell, all that matters is to distinguish, for each input velocity of the particle, between b output candidate target cells. This map is a discrete counterpart to the connection associated to the metric. It contains just the finite amount of information that needs to be attached to the cell in order to compute geodesics. It could in fact be pre-compiled into each cell, thereby yielding a cellular automaton with $b + 1$ internal states to code for presence and velocity, times b^b to code for the discrete connection.

8 Time versus space, precision

Geodesics have been popularized by General Relativity. General Relativity likes to put space and time on an equal footing. Numerical schemes for General Relativity ought to pursue that path, in particular it would be nice if the timeline of the computed geodesic were just $0, \Delta, 2\Delta, 3\Delta, \dots$ that is if a was equal to 1. In the scheme of Section 3, this choice leads to a cellular automaton of radius 1, which is appealing, but it also restricts to $b = 3^n$ the number of possible velocities. As we discussed in Section 6, this severely limits the number of motions that can be described. In the quantum setting, superpositions of basic velocities may compensate for this [6, 7, 3]. Classically, this is dramatic loss in precision. This is why, in Section 5, we took $a = 10^7$.

However, we also saw that a radius of $a' = 1$ can be obtained from a cellular automaton of arbitrary radius a simply by grouping each a^n hypercube of cells into one supercell. Each supercell now has an internal state in $\Sigma' = \Sigma^{a^n}$. Notice that keeping the position of the single particle within the hypercube is crucial. Otherwise, all the velocities of norm less than one supercell are rounded up to the center of the supercell—and so the increased precision in the velocities is not much use. Hence, Σ' is really just coding for a velocity amongst b possibilities, which is appealing... but also for the position of the single particle within the hypercube, which perhaps is not so satisfactory. After all, what this space grouping has done is really just to hide the discrepancy between the discretization step Δ and the computed geodesics timeline step $a\Delta$, by hiding some of spatial precision within the internal space of the supercells.

Hence, $a \gg 1$ appears to be fundamental requirement for precision. Notice that large values for a are better obtained by diminishing the discretization step Δ rather than augmenting the timeline step $a\Delta$, as we cannot hope to achieve a pseudo-elliptic trajectory with just a handful of velocity changes per revolution. Running the simulations, it was indeed observed that a large, for instance $a = 10^7$, yields increased stability. But only to some extent: after a while the number of possible velocities $b = (2a + 1)^n$ exceeds those which can be stored as a vector of machine-sized integers.

It also helps to fine-grain the discretization step Δ , keeping a constant. Running the simulations, it was indeed observed that this yields increased stability and convergence—at the expense of (reasonably) longer computation times. At some point, however, the finite-differences of (3) can become unstable, due to very small differences between $l(E, F, G)$ and $l(E, F', G)$ when $FF' = 1$, again hitting bounded machine floating point-arithmetic precision—but this can easily be fixed by evaluating these derivatives with FF' a fraction of $l(E, F, G)$ independent of Δ .

9 Recovering continuous spacetime geodesics

The algorithm of Section 3 is successful in computing geodesics in discrete time and space $\mathbb{Z} \times \mathbb{Z}^n$, in a way which is consistent with continuous-space discrete-time geodesics. We now explain how continuous-space discrete-time geodesics are

themselves consistent with the standard geodesics of the fully continuous setting. For this question to make sense, we place ourselves in the case of Section 4: a distance-induced deviation function.

As in Figure 4, consider three points E , F , G , taken at successive times $0, \tau, 2\tau$. Let ε be the distance EF , measured according to $g(E)$, that is the proper time along \mathbf{EF} and $v = \mathbf{EF}/\varepsilon$. In the same way, let ε' be the distance FG according to $g(F)$ and $v' = \mathbf{FG}/\varepsilon'$.

We said that trajectory EFG is a continuous-space discrete-time geodesics if and only if it minimizes the distance $EF + FG$, with respect to infinitesimal changes of F into F' . Let us take $FF' = \delta d$ where d is a vector, normal with respect to $g(F)$.

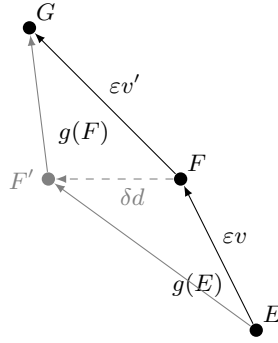


Fig. 4. The continuum limit is obtained for ε and δ tending to zero.

The distance $EF' + F'G$ is given by:

$$\sqrt{(\varepsilon v + \delta d)^\dagger g(E)(\varepsilon v + \delta d)} + \sqrt{(\varepsilon v' - \delta d)^\dagger g(F)(\varepsilon v' - \delta d)}$$

Consider the first term. Its derivative with respect to δ is

$$\frac{d^\dagger g(E)(\varepsilon v + \delta d) + (\varepsilon v + \delta d)^\dagger g(E)d}{2\sqrt{(\varepsilon v + \delta d)^\dagger g(E)(\varepsilon v + \delta d)}}$$

Taken at $\delta = 0$ and using the symmetry of $g(E)$ we get:

$$\frac{d^\dagger g(E)(\varepsilon v)}{\sqrt{(\varepsilon v)^\dagger g(E)(\varepsilon v)}} = d^\dagger g(E)v$$

Consider the second term. If $g(F')$ were just $g(F)$, the same process would yield $-d^\dagger g(F)v'$. We would then just have $d^\dagger g(E)v - d^\dagger g(F)v' = 0$, yielding $v' = g(F)^{-1}g(E)v$. This is the equation derived in [17], and is in the same spirit as that obtained [15] in the framework of simplicial complexes. Unfortunately it does not yield accurate predictions for perihelion shift, as pointed out in [17, 4]

and confirmed by our simulations. This is because one has to take into account that the variations of $g(F)$ around F yield a third term:

$$\frac{(\varepsilon'v')^\dagger(\partial g(F).d)(\varepsilon'v')}{2\sqrt{(\varepsilon'v')^\dagger g(F)(\varepsilon'v')}} = \frac{\varepsilon'}{2}v'^\dagger(\partial g(F).d)v'$$

Let us emphasize that straightest geodesics on simplicial complexes [15] do not see this term either: quite simply because a path EF between two adjacent simplices sees the geometry of the first simplex—that is the term $g(E)$ —and the geometry of the second simplex—that is the term $g(F)$ —, but ignores the variations of the geometry in some arbitrary direction FF' . In other words, simplices are usually thought of as polyhedrons of constant metric—but in order to be consistent with the continuum they must be interpreted as surfaces of constant metric derivatives. Altogether, we get that trajectory EF is a geodesics if and only if

$$d^\dagger(g(F)v' - g(E)v) = \frac{\varepsilon'}{2}v'^\dagger(\partial g(F).d)v' \quad (4)$$

in every directions d . Unfortunately, this is still inconvenient to solve for v' . At this stage the traditional, continuous approach to geodesics follows two simplifying steps, which in the discrete setting translate into two approximations. The first step is to evaluate the condition for d only along the coordinate directions:

$$(g(F)_\lambda.v' - g(E)_\lambda.v) = \frac{\varepsilon'}{2}v'^\dagger(g(F)_{,\lambda})v' \quad (5)$$

for all λ . The second step is to realise that $\mathbf{FG} = \mathbf{EF} + O(\varepsilon^2)$, and hence that $v' = v + O(\varepsilon)$ and $\varepsilon' = \varepsilon + O(\varepsilon^2)$. Indeed, in the continuum we assume that the time trajectory $x(t)$ is twice differentiable hence is has a first order expansion in τ , from which we get $\mathbf{FG} = \mathbf{EF} + O(\tau^2)$ and $EF \sim \tau \frac{dx}{dt}$, i.e. $\varepsilon \sim \tau$.

We get:

$$g(F)_\lambda.v' = g(E)_\lambda.v + \frac{\varepsilon}{2}v'^\dagger(g(F)_{,\lambda})v. \quad (6)$$

$$v' = g(F)_{,\lambda}^{-1} \left(g(E)_\lambda.v + \frac{\varepsilon}{2}v'^\dagger g(F)_{,\lambda}v \right) \quad (7)$$

We get:

$$\begin{aligned} g_\lambda.v' &= g_\lambda.v - \varepsilon g_{\lambda,\mu}v^\mu + \frac{\varepsilon}{2}v'^\dagger g_{,\lambda}v \\ g_\lambda.(v' - v) &= \frac{\varepsilon}{2} \left(v'^\dagger g_{,\lambda}v - 2g_{\lambda\nu,\mu}v^\mu v^\nu \right) \\ g_\lambda.(v' - v) &= \frac{\varepsilon}{2} \left(g_{\mu\nu,\lambda}v^\mu v^\nu - g_{\lambda\nu,\mu}v^\mu v^\nu - g_{\lambda\mu,\nu}v^\mu v^\nu \right) \\ (v' - v) &= -\varepsilon \Gamma_{\mu\nu}v^\mu v^\nu \end{aligned} \quad (8)$$

where

$$\Gamma_{\mu\nu} = g_{,\lambda}^{-1} (g_{\lambda\nu,\mu} + g_{\lambda\mu,\nu} - g_{\mu\nu,\lambda}) / 2 \quad (9)$$

Let us study the continuum limit $\varepsilon \rightarrow 0$. Suppose E, F, G were three consecutive points along a curve x parametrized by its proper-time s . Since ε was the proper time along EF , we have

$$\frac{dx}{ds} = \lim_{\varepsilon \rightarrow 0} \mathbf{EF} / \varepsilon = \lim_{\varepsilon \rightarrow 0} v$$

and

$$\frac{d^2x}{ds^2} = \lim_{\varepsilon \rightarrow 0} (\mathbf{FG} - \mathbf{EF}) / \varepsilon^2 = \lim_{\varepsilon \rightarrow 0} (v' - v) / \varepsilon$$

and hence

$$\frac{d^2x}{ds^2} = -\Gamma_{\mu\nu} \frac{dx^\mu}{ds} \frac{dx^\nu}{ds} \tag{10}$$

which is your traditional geodesics equation.

10 Conclusion

Summarizing, we have introduced a generic notion of discrete geodesics as straightest trajectories in discretized spacetime, which are such that any three successive points E, F, G must minimize the deviation function $w(E, F, G)$. Given E and F , G is implicitly determined: this can be viewed as a dynamical system and computed via a gradient descent algorithm. For a metric space, the canonical choice for $w(., ., .)$ measures how the length $EF + FG$ varies with small variation of F . This was validated numerically, by computing the trajectory of a planet in discretized Schwarzschild spacetime, and recovering a perihelion shift of the right order. This was also validated by taking the continuum limit and recovering the standard geodesics equations on pseudo-riemannian manifolds.

Part of our motivations were to evaluate the strength and limits of cellular automata. Recall that three well-accepted postulates about physics—bounded velocity of propagation of information, homogeneity in time and space, and bounded density of information—necessarily imply that physics may be cast in the framework of cellular automata—both in the classical and quantum settings [9, 1]. Both theorems, however, rely on the implicit hypothesis of a flat spacetime. To which extent can cellular automata account for relativistic trajectories, that is geodesics? This paper shows that discrete geodesics can be cast in the framework of cellular automata, provided that a few extra assumptions are met: that the metric can be given with bounded precision, and that it has the property of fixing a velocity limit. These extra assumptions do not contradict the three postulates: they are but instances of them.

Yet, this paper shows that a large discrepancy between the time discretization step the space discretization step is necessary in order to maintain a good precision on the velocity of particles. Namely, the number of particle velocities varies in $(2a + 1)^n$, with n the dimension of space and the radius a of the cellular automaton, which is therefore inherently large. Thus, computing discrete geodesics—and straight lines in euclidean space, for that matter—is local... but

not that local. This may come as a surprise, and suggest that geodesics equations are better-behaved in the continuum. An alternative is to live with imprecise velocities. A planet is a collection of particles, and so it may be the average of their imprecise velocities which grants it a precise averaged velocity. In fact, a single particle is itself quantum, and may thus be in a superposition of these imprecise velocities, yielding a precise averaged velocity—as is made formal in the eikonal approximation [5]. This is in fact precisely what happens in quantum cellular automata models of quantum particles in curved spacetime, as shown in [6, 7, 3]. All of these considerations suggest that nature’s way of working out timelike geodesics trajectories may in fact be emergent, from the simpler and more local behaviour of spinning particles.

Hence, for future work, it may be interesting to look for discrete models based on spinning particles, oscillating along a few, cardinal, light-like directions. These may in fact be closer to mimicking the real behaviour of fermions in curved spacetime, with the hope to recover the Mathisson-Papapetrou-Dixon equation—a generalization of the geodesics equation to spatially extended massive spinning bodies—as emergent, in analogy with the continuum [5]. Such discrete models may be more local. Another approach is to work directly in terms of a discrete connection [10]. In the continuum, the Levi-Civita connection is axiomatized as being the unique metric-compatible and torsion-free connection. That given in Equation (9) is exactly torsion-free, but interpreted as a discrete connection, as in Equation (8), it is metric-compatible only to first order. One can ask for both properties to be met exactly even in the discrete setting, this specifies the intersection of two ellipses. In 2-dimensions the number of solutions is finite, but this is not even the case in higher-dimensions: the axiomatization suggested by the continuum breaks down and demands fixing.

Acknowledgements

This work has been funded by the ANR-12-BS02-007-01 TARMAC grant, the ANR-10-JCJC-0208 CausaQ grant, and the John Templeton Foundation, grant ID 15619. Pablo Arrighi benefited from a visitor status at the IXXI institute of Lyon.

References

1. P. Arrighi and G. Dowek. The physical Church-Turing thesis and the principles of quantum theory. *Int. J. Found. of Computer Science*, 23, 2012.
2. P. Arrighi and G. Dowek. Discrete geodesics. *arXiv Pre-print, with program available when downloading source.*, 2015.
3. P. Arrighi, S. Facchini, and M. Forets. Quantum walks in curved spacetime. *Pre-print arXiv:1505.07023*, 2015.
4. L. Brewin. Particle paths in a schwarzschild spacetime via the regge calculus. *Classical and Quantum Gravity*, 10(9):1803, 1993.
5. F. Cianfrani and G. Montani. Dirac equations in curved space-time vs. papapetrou spinning particles. *EPL (Europhysics Letters)*, 84(3):30008, 2008.

6. G. Di Molfetta, M. Brachet, and F. Debbasch. Quantum walks as massless dirac fermions in curved space-time. *Physical Review A*, 88(4):042301, 2013.
7. G. Di Molfetta, M. Brachet, and F. Debbasch. Quantum walks in artificial electric and gravitational fields. *Physica A: Statistical Mechanics and its Applications*, 397:157–168, 2014.
8. Ray d’Inverno. *Introducing Einstein’s Relativity*. Oxford University Press, USA, 1899.
9. R. Gandy. Church’s thesis and principles for mechanisms. In *The Kleene Symposium*, Amsterdam, 1980. North-Holland Publishing Company.
10. M. Lorenzi, N. Ayache, and X. Pennec. Schilds ladder for the parallel transport of deformations in time series of images. In *Information Processing in Medical Imaging*, pages 463–474. Springer, 2011.
11. J.E. Marsden and M. West. Discrete mechanics and variational integrators. *Acta Numerica 2001*, 10:357–514, 2001.
12. D. Martínez, L. Velho, and P.C. Carvalho. Computing geodesics on triangular meshes. *Computers & Graphics*, 29(5):667–675, 2005.
13. J.S.B. Mitchell, D.M. Mount, and Ch.H. Papadimitriou. The discrete geodesic problem. *SIAM Journal on Computing*, 16(4):647–668, 1987.
14. G. Peyré, M. Péchaud, R. Keriven, and L.D. Cohen. Geodesic methods in computer vision and graphics. *Foundations and Trends in Computer Graphics and Vision*, 5(3–4):197–397, 2010.
15. K. Polthier and M. Schmies. Straightest geodesics on polyhedral surfaces. *Discrete Differential Geometry: An Applied Introduction. SIGGRAPH 2006.*, page 30, 2006.
16. F.H. Vincent, E. Gourgoulhon, and J. Novak. 3+1 geodesic equation and images in numerical spacetimes. *Classical and Quantum Gravity*, 29(24):245005, 2012.
17. R.M. Williams and G.F.R. Ellis. Regge calculus and observations. i. formalism and applications to radial motion and circular orbits. *General Relativity and Gravitation*, 13(4):361–395, 1981.